

Paired Distrometric Measurements in the South of Brazil: Wind Effects and Sampling Uncertainties

Roberto V. Calheiros¹, Cesar Beneti¹, Camila Oliveira^{1,2}, and Leonardo Calvetti³

¹SIMEPAR - Parana Meteorological Service, Brazil

²UFPR - Parana Federal University, Brazil

³UFPEL - Federal University of Pelotas, Brazil

(Dated: 22 June 2018)

1. Introduction

Drop size distribution (DSD) is basic for the analysis of the microstructure of rainfall, which is of primary importance for the remote sensing of precipitation. As well, DSD plays an important role e.g. in precipitation physics, numerical weather and hydrological modeling, telecommunications, agricultural and soil sciences. Reliable measurements of DSD are basic to the understanding of the microstructure of rainfall at a more advanced level of analysis.

Measurements of DSD are usually performed at ground level using distrometers; the OTT Parsivel instrument is one of the distrometers most widely used in validation and comparison of weather radars, which is the application of interest in this study. In fact, when distrometer is used in radar calibration, errors in the measurements can have a significant impact, e.g. in the coefficient and exponent of the derived relationships between rain rate and radar variables. DSD measurements are affected by uncertainties resulting from both the natural variability of rainfall and the sampling fluctuations, a situation inherent to the measurement of any physical process.

At a more advanced level of an analysis, these uncertainties must be considered quantitatively. In this paper the approach of Jaffrain and Berne (2011) is followed to characterize and quantify the sampling uncertainties in the measurements from OTT Parsivel distrometers deployed in the State of Paraná, Brazil. These instruments are associated with the operations of two long-range S band radars (TXS: 25.5053°S, 50.3613°W and CAS: 24.8700°S, 53.5293°W) covering regions of high socio-economical relevance with outstanding agro-industrial activities and energy production. In fact, these radar survey an area where more than 33% of the hydro-power energy in the country is generated.

In a previous work (Calheiros et al., 2017) the compatibility of the distrometer measurements with those from the radars and collocated rain-gages was verified. In section 2 the instrumental measurement setting and data characterization are presented. Wind impact on the measurements is explored in section 3; while results are presented in sector 4. Section 5 closes the paper with a summary, ongoing work, and conclusions.

2. Instrumental Setup and Data Processing

For the present work, available data were from two paired OTT Parsivel distrometers (hereafter DR1 and DR2) which were disposed perpendicularly to each other, in the N-S and E-W directions, as shown schematically in Fig. 1.

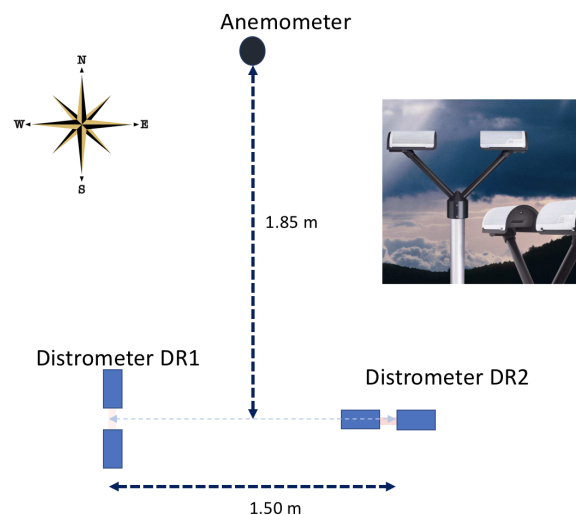


Figure 1: Schematic instrumental setup of the paired distrometers DR1 (N-S) and DR2 (E-W).

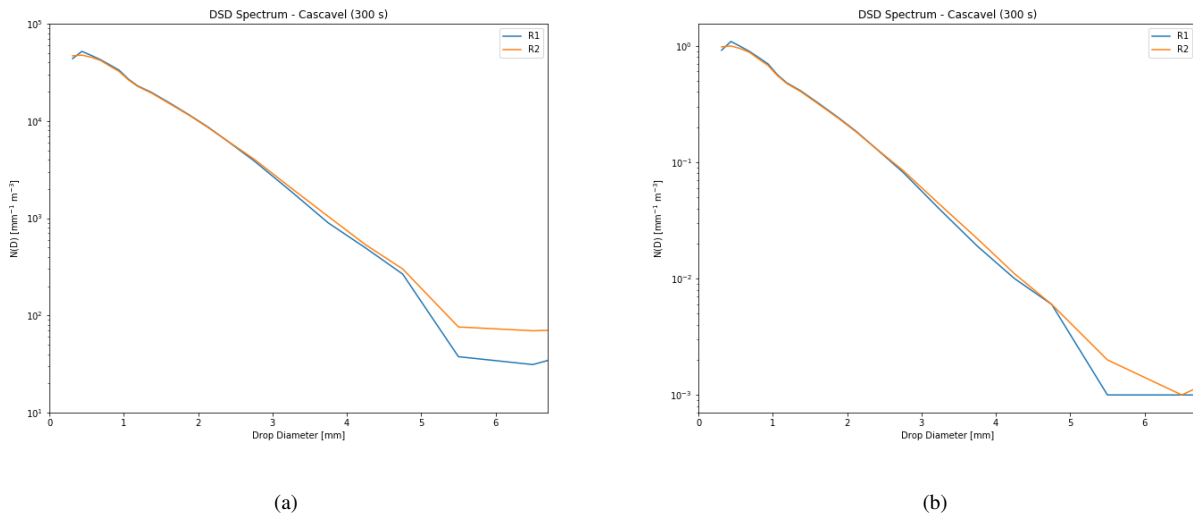


Figure 2: DSD spectra from DR1 and DR2 measurements for a time resolution of 300s (a) over the dataset period and (b) as an average over the period (21 Feb 2014 to 07 Aug 2014).

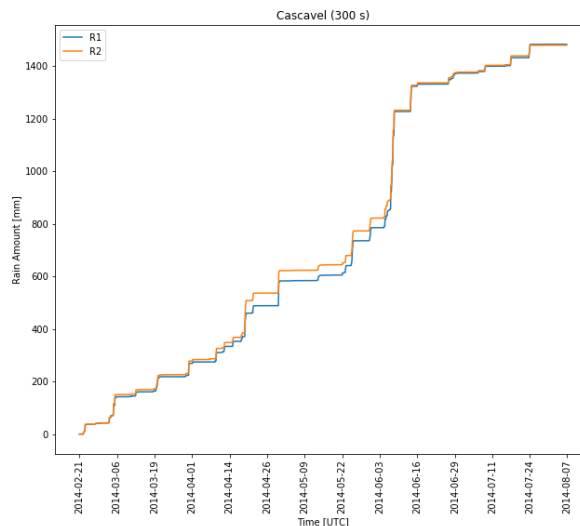


Figure 3: Rainfall from DR1 and DR2 at 300 s time resolution accumulated over the dataset period.

The instruments were collocated with the CAS radar. The dataset available from paired operations of the distrometers covered the period from 21 February 2014 to 07 August 2014 and data were recorded at a time resolution of 60 s in 32 diameter classes and 16 velocity classes. In Fig. 2 the DSD spectra measured by DR1 and DR2 at a time resolution of 300 s is shown.

DR1 spectrum shows a number concentration of drops slightly smaller than that from DR2, for a size diameter of about 2.5 mm and larger. Comparatively, the corresponding spectra from Jaffrain and Berne (2011) show the slight difference from a size diameter of 1.8 mm up to 5 mm). Fig. 3 present the rainfall accumulated by DR1 and DR2 during the dataset period, which amounts to approximately 1480 mm.

A comparison between the rain rates from DR1 and DR2 (R1 and R2 respectively) is presented in the scatterplot of Fig. 4.

In the previous work (Calheiros et al., 2017) before mentioned rain rates from DR1 covering a longer period at 900 s time resolution were compared to a collocated rain gage with comparable results. Time sequence of the differences R1-R2 covering the whole dataset period is presented in Fig. 5.

Characterization of the rainfall (Tokay et al., 2005) was performed based on seven major events selected from the study period and is presented in Table 1.

The scatterplot of the percent total difference of the rainfall accumulated by each distrometer (from RainTotal column in Table 1) in each event as a function of maximum rain rate is shown in Fig. 6.

There is indication of a possible trend, without considering event 6 which features an exceptional duration and extreme rainfall rate of 238 mm/h. It should be noted that Tokay et al. (2005), while working with a substantially higher number of

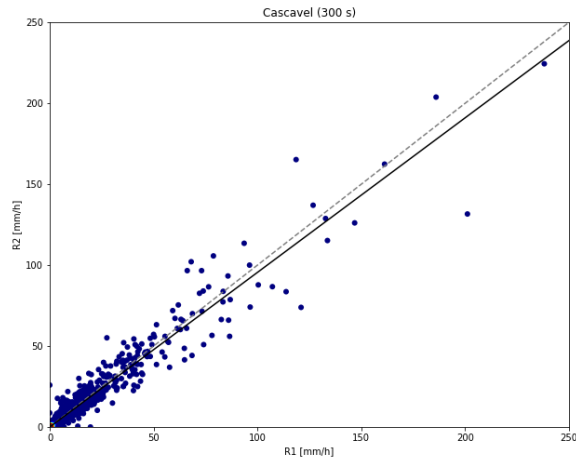


Figure 4: Dispersion diagram of rain rate R1 vs rain rate R2 at 300 s resolution, from measurements with DR1 and DR2, respectively.

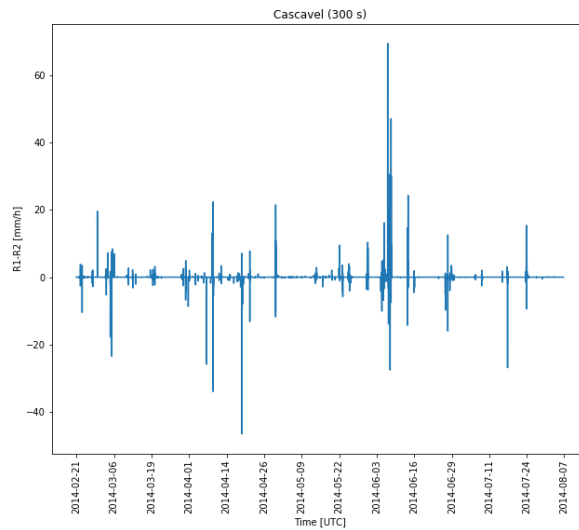


Figure 5: Temporal evolution of the difference between the 300 s resolution rain rates R1 and R2 covering the dataset period.

Table 1: Characterization of rainfall over DR1 and DR2 for seven major events during the dataset period.

Event	Date	Start Time (UTC)	End Time (UTC)	Rainy Minutes	Max Rain Rate (mm/h)	Rain Total (mm)	$ \Delta R_{total} $
1	05/03/14	17:35	18:10	40 – 40	96.6	28.6 – 31.5	2.9
2	09/04/14	16:05	20:10	250 – 245	102.1	32.1 – 37.5	5.4
3	19/04/14	09:40	20:10	560 – 565	165.2	88.9 – 121.9	33.0
4	30/04/14 – 01/05/14	20:00	09:10	600 – 565	137	94 – 85.2	8.8
5	07–08/06/14	09:00	17:15	1400 – 1395	238.1	371.4 – 339.8	31.6
6	14/06/14	01:00	10:15	540 – 540	68.5	95.8 – 94.9	0.9
7	17-18/07/14	18:50	04:00	400 – 405	105.7	30.1 – 33.6	3.5

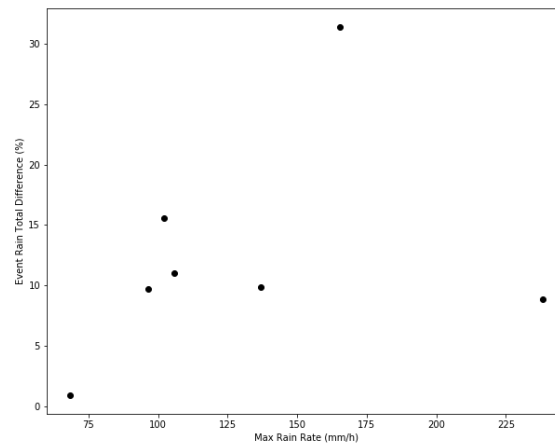


Figure 6: Scatterplot of percentual difference between the accumulated rainfall from DR1 and DR2 for the events in Table 1 as a function of maximum rain rate for the event.

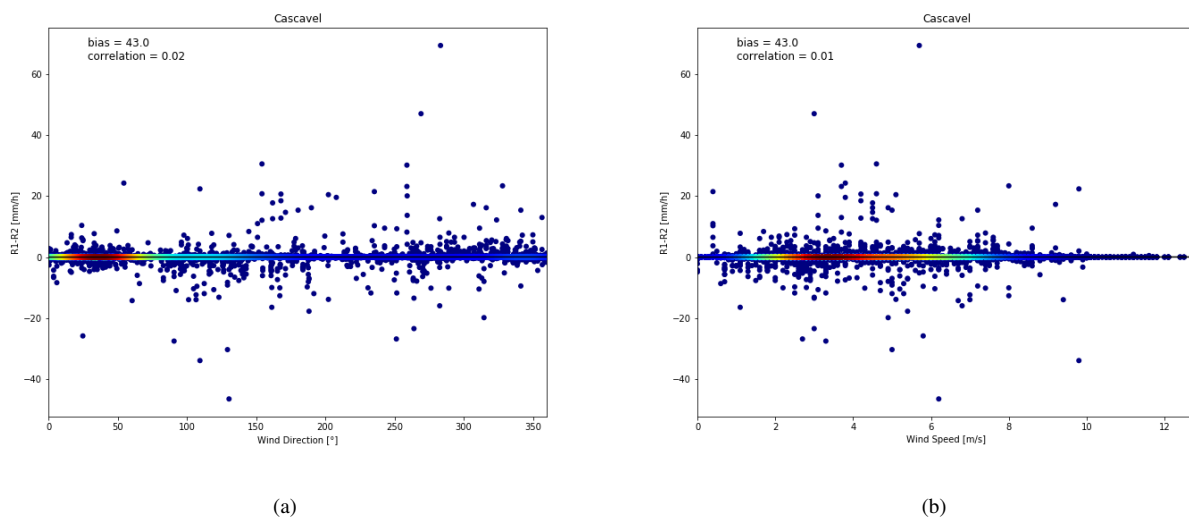


Figure 7: Difference between R1 and R2 (rain rates from DR1 and DR2, respectively) as a function of wind direction (a) and wind speed (b).

events, point out that “interestingly” such trend was not identified. Also, in comparisons with their work, it should be noted that they used a different kind of distrometer, i.e., the JW impact instrument.

3. Wind Effects

Scatterplots of R1-R2 vs wind direction and wind speed, as shown in Fig. 7 (a) and (b), were elaborated which have shown correlations coefficients of 0.02 and 0.01, respectively. These values are comparable to those of Jaffrain and Berne (2011) who obtained correlation coefficients of -0.05 and -0.08.

While, in general, these results do not indicate a significant influence of the wind on the difference between the measurements from the distrometers, the noticeable number of cases featuring substantial deviations prompted further investigation, in the context of this preliminary work. A first verification following the work of Tokay et al. (2005) considering whole events was performed by taking the events characterized in Table 1 and elaborating a scatterplot of the percent total differences of rainfall accumulated by DR1 and DR2 vs the mean wind speed for each event, as depicted in Fig. 8.

While impaired by the small number of events when compared with theirs, the percent differences obtained in the present work are compatible with those for most (80%) of their events. As shown in the scatterplot six of the seven events presented percent differences in the total accumulation under 20%; for the remaining event percent difference was 23%. A second verification was undertaken, now for individual cases of 300 s time resolution rain rates, i.e. R1 and R2, selected from the seven events of Table 1. Cases are characterized in Table 2. Only cases of high rain rates equal to or exceeding 90 mm/h and with a percent difference between R1 and R2 exceeding 10% were selected.

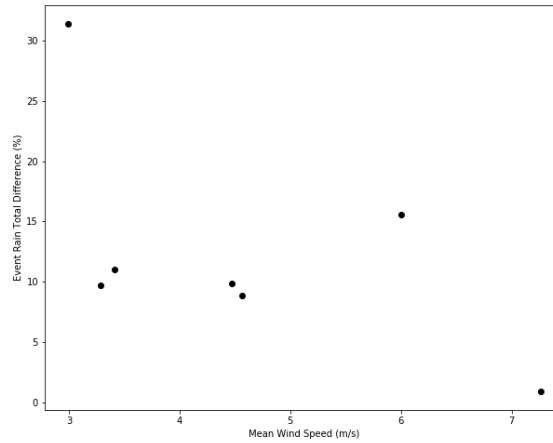


Figure 8: Scatterplot of percentual difference between the accumulated rainfall from DR1 and DR2 for the events in Table 1 as a function of mean wind speed for the event.

Table 2: Cases of rainfall at 300 s resolution from the seven major events in Table 1 when rain rate was equal to or bigger than 90 mm/h and percent difference between R1 and R2 exceeded 10%.

Case	Date	Rmax (mm/h)	Wind Direction (°)	Gust Wind (m/s)	R1-R2 (%)
1	05/03/14 17:50	96.6	264.1	9.1	27.7
2	09/04/14 16:25	102.1	109.5	14.5	40.0
3	09/04/14 16:30	96.5	109.5	14.5	26.3
4	19/04/14 10:10	113.5	314.7	19.1	19.2
5	19/04/14 12:20	165.2	130.5	9.3	32.8
6	19/04/14 12:50	96.6	129.4	8.3	37.3
7	07/06/14 10:20	201.1	283.3	11.1	41.8
8	07/06/14 17:30	107.2	202.3	8.8	21.1
9	07/06/14 20:40	146.8	168.0	6.7	15.2
10	07/06/14 20:45	133.7	168.0	6.7	14.9
11	08/06/14 04:45	100.4	162.0	7.8	13.4
12	08/06/14 13:35	121.0	269.2	5.0	48.3
13	08/06/14 14:55	113.8	259.0	7.9	30.6
14	17/07/14 22:50	105.7	251.4	8.2	29.2

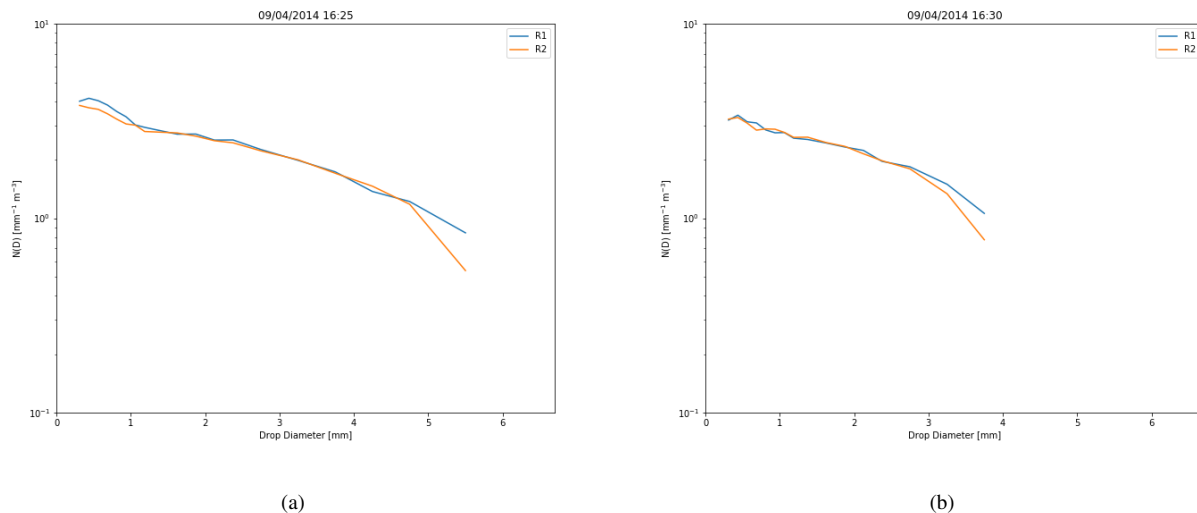


Figure 9: DSD spectra for 300 s time resolution from DR1 and DR2 for (a) 09/04/2014 at 16:25 and (b) 16:30h LT (UTC).

Table 3: Relative sampling uncertainty σ_ϵ and σ_ω (relative) as defined in Jaffrain and Berne (2011) for the paired DR1 and DR2 (one collocated distrometer) as a function of time resolution for rain rate values in the interval $[0.1, 2]$ mm/h.

Time Step	σ_ϵ	σ_ω
60	0.24	0.34
300	0.21	0.29
600	0.16	0.23
900	0.12	0.17

In 79% of the cases, the angle between the wind direction and the direction of the distrometer laser beam axis (N-S for DR1 and E-W for DR2) varied between 6° and 22° , i.e. the wind was nearly aligned with one the beams. In 71% of the cases, in which the percent difference $|R1-R2|$ was varying between 19% and 41.8%, gust winds varied between 7.9 and 19.1 m/s. In their paper Friedrich et al. (2013) explore the influence of strong winds on the quality of Parsivel measurements, based inclusive on data from convective thunderstorms during the VORTEX2 experiment. They investigate an artifact characterized by a large concentration of raindrops with large diameter and unrealistic fall velocities, which is correlated to high wind speeds. Regarding the VORTEX2 data they report that in strong winds, i.e. $> 7\text{ m/s}$ large particles with size diameter $> 6\text{ mm}$ are characteristic in the histograms. They comment that in addition to wind speed, the wind direction in relation to the laser beam axis orientation may also affect measurement. Also, they inform that the manufacturer recommends that the Parsivel be oriented with the laser beam axis perpendicular to the wind. In an early verification, in the context of the present study, a set of spectra from DR1 and DR2 from two cases in Table 2, e.g. 09/04/2014 at 16:25 h UTC and 16:30 h UTC, were generated. Mean wind speed was 9.8 m/s and wind gust was 14.5 m/s; percent differences between distrometer rain rates were 40% and 26.3% respectively. Spectra are shown in Fig. 9 (a) and (b); it is noted that larger raindrops size diameter goes from about 5.5 mm to about 3.8 mm and the number concentration decrease throughout the full range of size diameters as the maximum rain rate goes from 102.1 mm/h to 96.5 mm/h to 21.3 mm/h (not shown) and the wind speed goes from 9.8 m/s to 7.2 m/s (not shown) and wind gusts from 14.5 m/s to 11.0 m/s (not shown).

4. Sampling Uncertainty Results

For quantification of the sampling uncertainty the moments of DSD, i.e. rain rate R and ZH (radar reflectivity at horizontal polarization) were used (Tokay et al., 2002, 2005). ZH and ZDR were computed for S band. The methodology of Jaffrain and Berne (2011) was followed and, as in Tokay et al. (2005), it was considered that DR1 and DR2 sample the same population of droplets. The relative sampling uncertainty, as defined by the authors (see their Eq. 14), is calculated for R considering one collocated station (see their Fig. 9), which is the case in this study, for the same R interval as theirs, for different values of time resolution; results are presented on Table 3.

The computation of the relative sampling uncertainty is then extended to different classes of R up to 90 mm/h, covering most of existing values of rain rate. Results are presented as a set of curves of uncertainty as a function of class and time resolution. Class width was defined to include a minimum of 30 samples, considering a reliable quantification of the uncertainty. Since time resolution affects substantially the relative uncertainty several values were used from 60 s (as set in DR1 and DR2) to 2000 s. Because of assumptions of Gaussian distribution in the methodology of Jaffrain and Berne (2011) a verification was performed using one class of R , for a specific time resolution, as shown in Fig. 10.

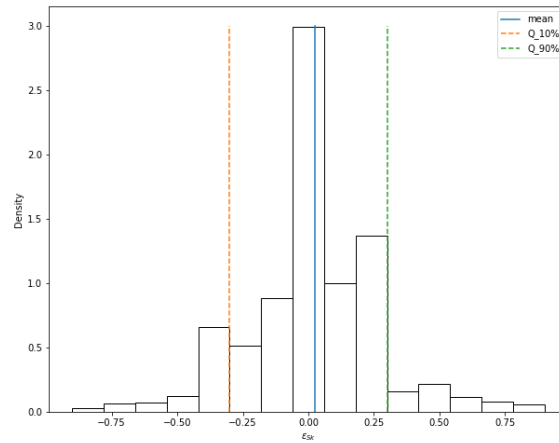


Figure 10: Rain rate value distribution for the interval [0.1, 2] mm/h at a time resolution of 60 s.

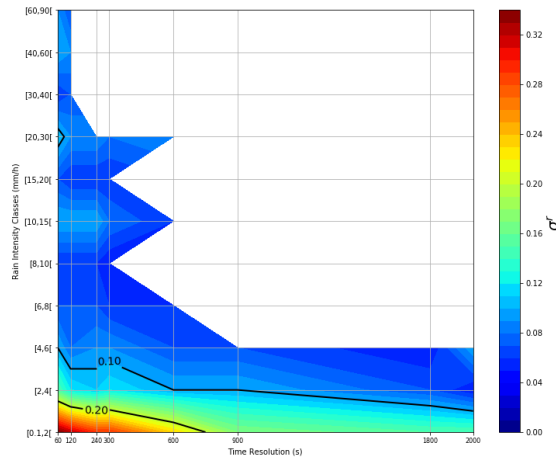


Figure 11: Relative sampling uncertainty for estimates of rain rate as a function of rain rate and time resolution.

Similarly to the finding of the authors, the assumption looks acceptable. The results for the sampling uncertainty on R estimates are shown in Fig. 11.

The relative sampling uncertainty varies between about 4% and 34%. In general, it increases with the increase of the order of the class and the increase of time step. There are three relatively small inhomogeneity areas in this general pattern for time resolution between 60s and 300s. The first is around the 15 mm/h level line where uncertainty rises to 10%, the second is around the 30 mm/h level where uncertainties exceeds 10%, and the third is around the 60 mm/h level line from time resolution of 60s to 120s where uncertainty is again 10%. For time step of 300s and lower the uncertainty is below about 10%-11% for all R values above approximately 5-6 mm/h and between about 10% and 34% from 5-6 mm/h down to the lowest rain rate. From time step of 300s and higher the general pattern of decreasing uncertainty with increasing rain rate and increasing time step is followed Fig. 12 shows the relative sampling uncertainty associated to the estimates of radar reflectivity at horizontal polarization (ZH), for the indicated classes of reflectivity (dBZ) and time resolution.

The sampling uncertainty isoline of 5% descends gradually from 25 dBZ to 20 dBZ, from time resolution of 60s to 120s. Uncertainty increases to about 19% at the 10 dBZ level line for all values of time resolution. Down from 10 dBZ to the 0 dBZ level line the uncertainty increases to about 50%-60% for all time resolution. Above about 10 dBZ, the general pattern shows a decrease of uncertainty from 19% to less than about 3%. There is a relatively small inhomogeneity in this pattern, in the upper portion of the map, from about 35 dBZ to 40 dBZ and from time resolution of 600s to 1800 s, where uncertainty increases to about 4%-5%.

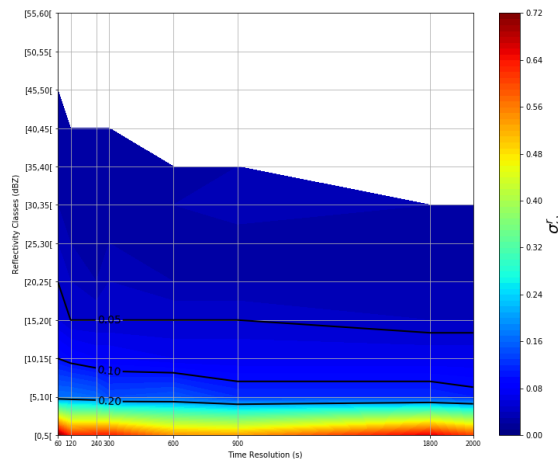


Figure 12: Relative sampling uncertainty for estimates of radar reflectivity ZH from [DR1, DR2 > definir] at S band as a function of ZH and time resolution.

5. Comments and conclusions

The Parsivel distrometer is one of the instruments for measurements of DSD at the ground level most widely used as a support to calibration of weather radars. Differences in the distrometer measurements affect the coefficient and exponent of the derived radar rainfall algorithms. The quantification of the variability of DSD measurements is of paramount importance for radar based precipitation estimation, among other environmental applications. The variability resulting from the sampling process of DSD measurement must be taken into account for a reliable quantification of the variability of DSD. This issue is dealt with in this study following Jaffrain and Berne (2011), is based on a dataset from a different climate and extends their work to heavy precipitation. Wind effects were considered and while in general influences were not significant, a noticeable number of cases with substantial differences led to further verification. Rainfall characterization was performed with major events and differences between distrometer measurements from the events as a function of mean wind speed were mostly within 20%, a result comparable to Tokay et al. (2005). Individual cases within the events, with high rain rates and significant differences between the measurements from the distrometers, were considered. In 71% of the cases the wind direction and the long axis of the distrometer were nearly aligned, and wind gusts were between 7.9 m/s and 19.1 m/s. DSD spectra for two selected sequential cases from the major events, featuring high wind speeds and differences between distrometer measurements were verified. It is noted that larger drops size diameter decreases from approximately 5.5 mm to 3.8 mm when rain rates and wind speeds decrease significantly. The relative sampling uncertainty related to the estimates of rain rate (R) and reflectivity at horizontal polarization (ZH) were quantified. For R the uncertainty ranged from approximately 4% to 32%; the general pattern is of decreasing uncertainty with increasing values of rain intensity and increasing time resolution. Uncertainty is below about 11% for a time resolution of 300 s and lower and for rain rate at or above 5 to 6 mm/h; for rain rates below 5 to 6 mm/h and 0.1 mm/h uncertainty is between 10% and 34%. There are three inhomogeneity areas in the general pattern between time step of 60 s and 300 s, at around 15 mm/h with uncertainty of about 10%, at around 30 mm/h with uncertainty exceeding 10% and at around 60 mm/h from time step of 60 s and 120 s with uncertainty of 10%. For ZH the uncertainty varied between about 3% and 60%. The general pattern shows uncertainty gradually decreasing with increasing ZH and for all time steps, from 19% at the 10 dBZ level to about 3%. Between about 10 dBZ and 0 dBZ level lines uncertainty increases to about 50-60. There is a relatively small inhomogeneity in the uncertainty map within about 35-40 dBZ and 600–1800 s. The preliminary results regarding wind effects suggest that further investigation should be undertaken. The patterns of sampling uncertainty maps for R and ZH are, in general, comparable. The maps are, on the whole, compatible with the corresponding maps of Jaffrain and Berne (2011). The results related to the quantification of uncertainty suggest that the extension of their approach to the heavy rainfall in this study is valid. On going work includes exploring a larger number of events and cases for wind effects and quantification of uncertainty for ZDR and KDP.

References

- R. V. Calheiros, C. Oliveira, C. Beneti, and L. Calvetti, "Distrometric Drop Size Distribution in South Brazil: Derived Z-R Relationships and Comparisons with Radar Measurements," in *38th Conference on Radar Meteorology*, 2017, p. Paper 1.1.
- K. Friedrich, S. Higgins, F. J. Masters, and C. R. Lopez, "Articulating and stationary parsivel disdrometer measurements in conditions with strong winds and heavy rainfall," *Journal of Atmospheric and Oceanic Technology*, vol. 30, no. 9, pp. 2063–2080, 2013.



- J. Jaffrain and A. Berne, “Experimental quantification of the sampling uncertainty associated with measurements from parsivel disdrometers,” *Journal of Hydrometeorology*, vol. 12, pp. 352–370, 2011.
- A. Tokay, A. Kruger, W. F. Krajewski, P. A. Kucera, and A. J. Pereira Filho, “Measurements of drop size distribution in the southwestern amazon basin,” *Journal of Geophysical Research*, vol. 107, no. D20, 2002. [Online]. Available: <https://doi.org/10.1029/2001jd000355>
- A. Tokay, P. G. Bashor, and K. R. Wolff, “Error characteristics of rainfall measurements by collocated joss waldvogel disdrometers,” *Journal of Atmospheric and Oceanic Technology*, vol. 22, no. 5, pp. 513–527, 2005. [Online]. Available: <https://doi.org/10.1175/JTECH1734.1>